Far-wing collisional redistribution of light in the barium-rare gas systems

Ni, SY; Goetz, W; Meijer, HAJ; Andersen, N

Published in:
Zeitschrift für Physik. D: Atoms Molecules and Clusters

DOI:
10.1007/s004600050095

Publication date:
1996

Z. Phys. D 38, 303–308 (1996)

ZEITSCHRIFT
FÜR PHYSIK D

Far-wing collisional redistribution of light in the barium-rare gas systems

S.Y. Ni*, W. Goetz, H.A.J. Meijer, N. Andersen**

Niels Bohr Institute, Ørsted Laboratory, Universitetsparken 5, DK-2100 Copenhagen, Denmark

Received: 28 May 1996

Abstract. We have measured intensity and polarization of far-wing collisionally redistributed light from Ba perturbed by He, Ne, and Kr in a heated cell ($T \sim 800$ K). Collisional alignment decay rates were also determined. The light was detuned $\pm 3 - 900\ \mathrm{cm}^{-1}$ from the 5535 Å BaI $6^1S - 6^1P$ resonance line. The rare gas pressure was about 5 mbar. Together with the earlier data of Alford et al. [24], the results form a complete set of data for comparison with forthcoming predictions based on state-of-the-art theory for potential curves of Ba-rare gas systems. With emphasis on systematical trends, the results are discussed in terms of earlier theoretical and experimental findings for similar two-electron systems.

PACS: 32.70

1 Introduction

Since the pioneering experiments of Carlsten et al. [1] on collisional redistribution of light in the Sr-Ar system, many experimental and theoretical studies have demonstrated the kind of information that can be obtained from investigations in this area of optical collision studies. Briefly, in this technique near-resonant light with frequency ω_L and polarization $\hat{\varepsilon}_L$ from a tunable laser is shined on atoms surrounded by perturbers at single collision conditions. For weak laser intensities the scattered light has two components, Rayleigh scattered photons at ω_L and photons at the atomic resonance frequency, ω_o. The physics of this second component is the following. During an atom-perturber encounter, the atomic energy levels may come into resonance with the incident light at some internuclear distance (the Condon point R_C) at which the collision complex may become excited. This distance is thus controlled through the detuning $\Delta\omega = \omega_L - \omega_o$. When the quasi-molecule breaks up, the atom is left in an excited state which subsequently fluoresces. The redistribution coefficient, which is a measure of the intensity of the redistributed light, depends sensitively on the shape of the relevant molecular potential curves, in much the same way as the traditional absorption coefficient, or line-shape. In addition to the angular momentum quantum numbers of the relevant molecular states, the (linear or circular) polarization of the redistributed light depends on details of the collision dynamics, such as the distance, or decoupling radius R_{dec}, at which the molecule-to-separated atoms – transition takes place and thus contains information not accessible in traditional line-shape experiments.

The general theory of collisional redistribution is well developed [2–4], see also the review by Burnett [5]. For the polarization in particular, following the investigations by the JILA group [6, 7], a simple model for interpretation was proposed by Lewis et al. [8]. Here the polarization effects are described in terms of reorientation of the excited molecular orbital, which stays locked to the rotating internuclear axis from the excitation at the Condon point until the distance determined by the decoupling radius is reached, from which on the orbital stays fixed in space until the optical decay. Assuming straight line trajectories, for the cases of Σ and Π molecular potential curves the resulting polarizations can be evaulated in closed form and depend on the ratio R_C/R_{dec} only. For fixed decoupling radius R_{dec}, the polarizations decrease with decreasing excitation radius, R_C. For excitation to a Σ curve, the corresponding limiting polarization values are 32% ($R_C = R_{\mathrm{dec}}$) and 0% ($R_C \ll R_{\mathrm{dec}}$), respectively. For excitation to a Π curve, they are 67% ($R_C = R_{\mathrm{dec}}$) and 27% ($R_C \ll R_{\mathrm{dec}}$), respectively. The effects of bent trajectories, relevant for strong collisions at large detunings, are easily visualized and estimated within this model, using a hard sphere potential. The bending causes an increase of the polarization compared to that for a straight line trajectory, since the reorientation of the excited orbital

* *Permanent address*: Physics Department, Guizhou Institute for Nationalities, Guiyang, Guizhou, People's Republic of China
** *Permanent address*: Centrum voor Isotopen Onderzoek, Nijenborgh 4, 9747 AG Groningen, The Netherlands

is reduced. The degree to which the model holds has been investigated in a series of illuminating theoretical studies [9–12]. Most studies have addressed $S \rightarrow P$ or $J = 0 \rightarrow J = 1$ transitions in alkali atoms or alkaline-earth atoms, perturbed by rare gases.

For the alkali atoms, potential curves of good accuracy are known for several systems, but the collision dynamics is complicated by the effects of electron and nuclear spins, causing fine-structure splitting and hyperfine-structure depolarization. Nevertheless, a series of experimental and theoretical investigations have been completed with very satisfactory results [13–21], in particular for the Na-Ar system, for which the first polarization results for collisionally redistributed light were reported [13]; see also [22].

For the alkaline earth atoms, experiments have been done near the resonance transition for Ca [23], Sr [6, 7] and Ba [24–27]. The Ba-Ar, Xe experimental data form the most extensive set, exploring in detail the correlation between structures in the redistribution coefficient and the linear polarization [24], the circular polarization [25], and temperature effects [27]. The role of quasi-bound states has also been investigated [28]. Despite the simpler physics of these systems, lack of accurate potential curves has until now been a hindrance for systematic benchmark tests of theory.

Thanks to the improved sensitivity of a new experimental approach, results have recently become available over a wide range of detunings for the experimentally difficult Hg-Kr system [29, 30], for which good potential curves exist from Gryzuk's group [31, 32].

Theoretical progress has, however, recently enabled calculation of accurate potential curves for a series of two-electron atoms using pseudopotential methods [33, 34], including also the Ba-He system [35], and results for other rare gases seem within reach [36]. This has motivated the present experimental study, aimed at completing the data set of Alford et al. [24], by making available a full set of far-wing redistribution coefficients and linear polarizations for the rare gases. It is our hope that a systematic comparison thereby will become possible with theoretical predictions based on the new potential curves [36].

Below, we first describe our experimental setup and procedure for data evaluation. Section 3 presents results and discusses their main features in comparison with earlier experimental and theoretical results in the literature for similar systems.

2 Experimental setup and procedure

2.1 The setup

The experimental setup shown in Fig. 1 is similar to the one of Alford et al. [24], so only a brief outline is given. A CW dye laser (Coherent CR 590), pumped by an argon ion laser (Coherent Innova 90-5), is tuned near the BaI $6\ ^1S - 6\ ^1P$ resonance line at 5535 Å. After rotating the linear polarization into the plane of the table by means of a $\lambda/2$-plate, the light is sent through two dispersing prisms and a slit in order to remove the weak fluorescence

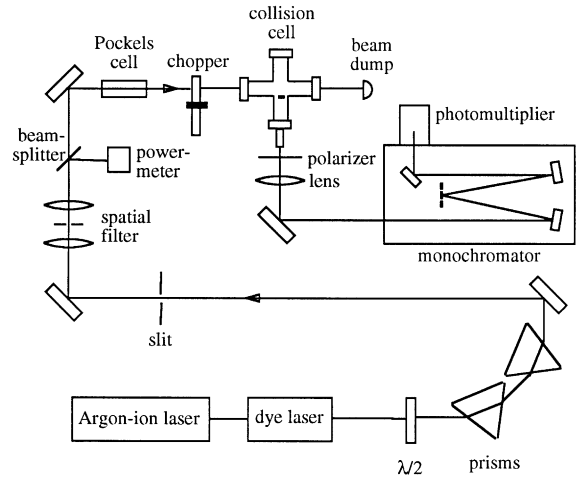

Fig. 1. A schematic diagram of the experimental setup

background from the dye (Rhodamine 110). After spatial filtering the light is sent through a Pockels cell, passes a chopper and enters the collision cell. The cell is a stainless steel cross, temperature controlled within 1 K in the 300-1000 K region and contains the buffer gas at a typical pressure of 5 mbar. The rare gas pressure is monitored with a capacitance manometer (Baratron model 221A) and can be varied in the 0-100 mbar region. Barium vapor comes from a solid piece of the metal placed in a side arm. The light emitted from a 1 cm section of the beam in the center of the cell passes through a sapphire window (cut perpendicular to the optical axis to avoid polarization distortion) mounted very close to the beam path in order to avoid trapping effects. The light intensity is monitored through a polarizer with transmission direction perpendicular to the beam. The beam section is imaged onto the entrance slit of a .67 m monochromator (McPherson model 207) and detected by a cooled photomultiplier (EMI 9893Q), the output of which is sent to a computer controlled photon-counting system. The monochromator separates the fluorescence signal from the Rayleigh scattered light, and the actual value of the detuning $\Delta\omega$ is determined by scanning. The polarization of the fluorescence is measured by rotating the polarization direction of the incident beam by the Pockels cell, thereby eliminating systematic errors due to polarization dependence of the detection efficiency, and possible beam displacements introduced if a rotatable polarizer were used. The chopper allows separation of the signal from background photons due to e.g., the heated cell. The laser power in the cell was 100-300 mW, depending on detuning and chemical degradation of the dye.

2.2 Pressure depolarization

Due to the finite pressure of the buffer gas, the light polarization is reduced due to elastic collisions of the excited, aligned Ba atoms with perturber atoms before the optical decay. This effect is corrected for by measuring the pressure dependence of the polarization and extrapolating the results to zero pressure in the following way.

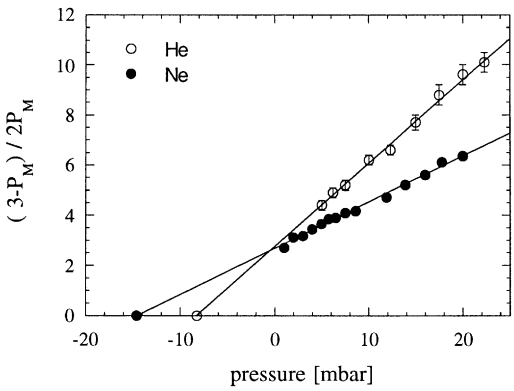

Fig. 2. Variation of the alignment parameter, Eq. (1), with perturber pressure for He ($\Delta\omega = 8.6\ \mathrm{cm}^{-1}$) and Ne ($\Delta\omega = -27.3\ \mathrm{cm}^{-1}$)

Table 1. Collisional alignment decay rates $\gamma_c^{(2)}/N_p$ (in $10^9\ \mathrm{cm}^3\,\mathrm{s}^{-1}$) for Ba-rare gas and Sr-rare gas systems

Perturber	Ba (this work)	Ba [24]	Sr [7]
He	1.67 ± 0.25	–	1.66 ± 0.28
Ne	1.01 ± 0.12	–	0.88 ± 0.08
Ar	1.33 ± 0.19	1.30 ± 0.08	1.58 ± 0.19
Kr	1.41 ± 0.11	–	1.91 ± 0.39
Xe	1.38 ± 0.15	1.42 ± 0.09	2.00 ± 0.31

The pressure dependence of the alignment parameter β is [3]

$$\frac{1}{\beta} = \frac{3 - P_M}{2P_M} = \frac{1}{\alpha_M^{(2)}(\omega_L)}\left[1 + \frac{1}{\gamma_N}\frac{\gamma_c^{(2)}}{N_p}N_p\right]. \tag{1}$$

Here $\tau_N = 1/\gamma_N = 8.37$ ns is the lifetime of the BaI 6 ^1P level, $\gamma_c^{(2)}/N_p$ is the alignment decay rate, and N_p is the perturber density. Equation (1) predicts a linear dependence of $(3 - P_M)/2P_M$ with rare gas pressure. The slope depends on $\Delta\omega$, while the intercept with the abscissa does not.

Figure 2 shows examples of such measurements for Ba-He at a detuning of $\Delta\omega = 8.6\ \mathrm{cm}^{-1}$ and Ba-Ne at a detuning of $\Delta\omega = -7.3\ \mathrm{cm}^{-1}$. Temperatures were in the 700–800 K region. Due to surface coating of the barium piece, there is no unique relationship between Ba density and temperature. Our values for the alignment decay rates are given in Table 1. They compare well with the earlier values of Alford et al. [24]. Results for the Sr-rare gas systems [7] display a similar systematics and are shown for comparison.

2.3 Hyperfine structure depolarization

Of naturally abundant barium, 18% have nuclear spin $I = \frac{3}{2}$, with $I = 0$ for the rest. While the nuclear spin plays no role during the collision, the hyperfine structure develops almost fully before the optical decay, causing a reduction of the polarization. A detailed analysis yields the following relation between the actual (zero-pressure) polarization P_0 and the polarization P obtained if no hfs effects were present [24]

$$P = P_0 \Big/ \left[1 - q\frac{113}{450}(3 - P_0)\right] \tag{2}$$

where $q = 0.18$ being the fraction of atoms of $I = \frac{3}{2}$. The zero-pressure polarizations have been corrected according to this formula.

2.4 Absolute values of k_r

Alford et al. [24] used the Rayleigh scattering to bring their redistribution coefficients for Ba-Ar, Xe on an absolute scale. The error bars with this procedure were estimated to $\pm 20\%$, the main source of uncertainty being the background from photons scattered from the collision cell. More recently, Maeyama et al. [37] measured accurate blue far-wing absorption coefficients for all the rare gases using a Mach-Zehnder configuration setup. In the far blue wings, the two coefficients, redistribution and absorption, should be identical (no quasi-bound states), and the two sets of data [24, 37] indeed agree within the quoted error bars. Thus, for consistency, we have used the blue-wing results of [37] to establish our absolute scale. It will be seen in the next section that the curve shapes of [37] in the blue wing agree excellently with the present results, lending confidence to the procedure.

3 Results and discussion

Figures 3–7 show the line shapes and polarizations for Ba perturbed by He, Ne, Ar, Kr, and Xe, respectively. The

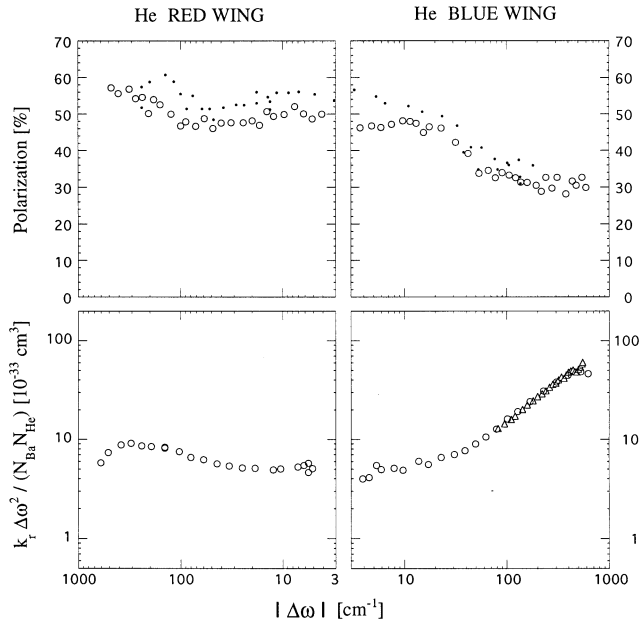

Fig. 3. Red and blue wing linear polarization and redistribution coefficient for the Ba-He system. (○) Present results; (△) blue wing absorption coefficient [37]; (·) polarization for Sr-He [7]

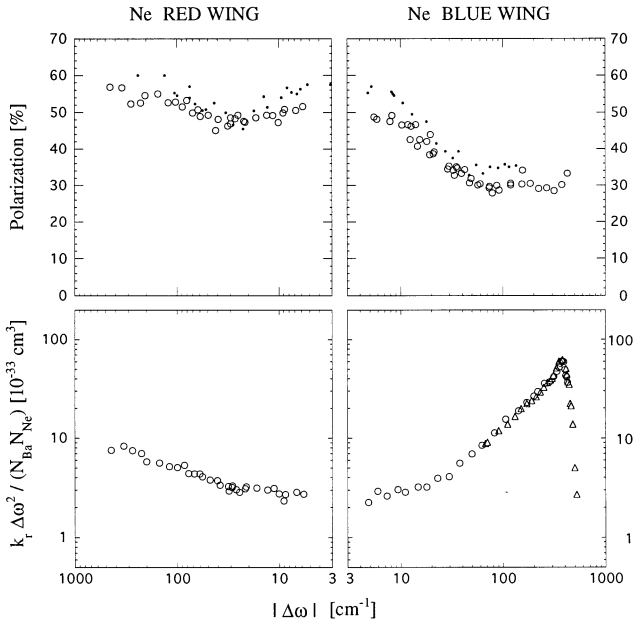

Fig. 4. Red and blue wing linear polarization and redistribution coefficient for the Ba-Ne system. (○) Present results; (△) blue wing absorption coefficient [37]; (·) polarization for Sr-Ne [7]

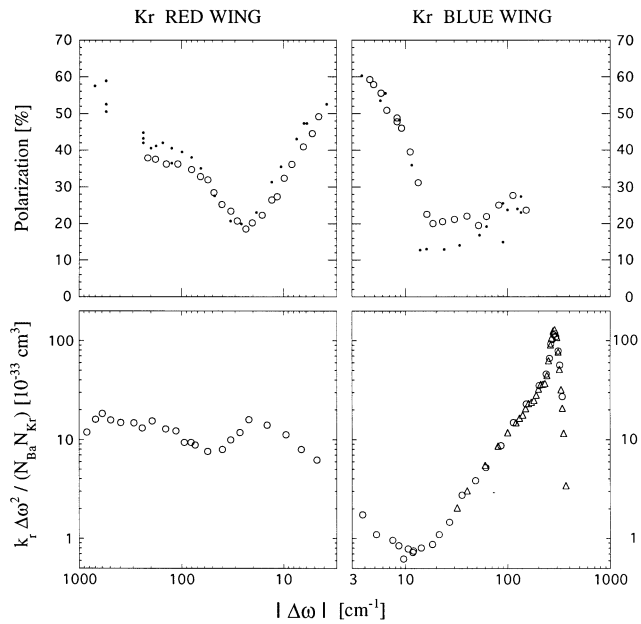

Fig. 6. Red and blue wing linear polarization and redistribution coefficient for the Ba-Kr system. (○) Present results; (△) blue wing absorption coefficient [37]; (·) polarization for Sr-Kr [7]

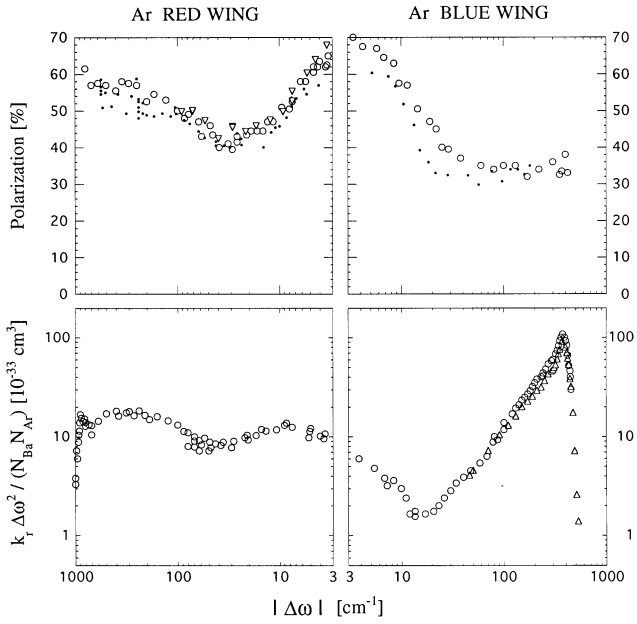

Fig. 5. Red and blue wing linear polarization and redistribution coefficient for the Ba-Ar system. (▽) Present results; (○) [24]; (△) blue wing absorption coefficient [37]; (·) polarization for Sr-Ar [7]

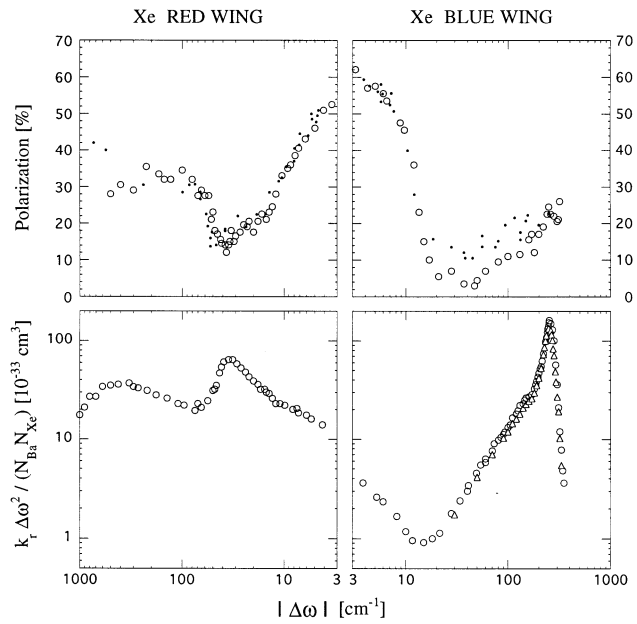

Fig. 7. Red and blue wing linear polarization and redistribution coefficient for the Ba-Xe system. (○) [24]; (△) blue wing absorption coefficient [37]; (·) polarization for Sr-Xe [7]

data shown are from the present work for Ba-He, Ne and Kr, from [24] for Ba-Ar, Xe, blue-wing line shapes from [37], and Sr-rare gas polarizations from [7], as indicated. In addition, we measured some red wing polarizations for Ba-Ar to check the consistency of our data with the earlier results of Alford et al. [24]. In all cases agreement was found within the quoted uncertainties.

3.1 Line shapes

In the figures, the redistribution coefficients $k_r(\Delta\omega)$ have been multiplied by $\Delta\omega^2$, the product $k_r(\Delta\omega)\Delta\omega^2$ being proportional to $\gamma_c(\Delta\omega)$, the frequency-dependent collision rate [2]. In this representation a Lorentzian line shape will yield a horizontal line, and satellite structures are clearly displayed.

First of all, we note a general, excellent agreement between our line shapes and the ones measured by Maeyama et al. [37] in an absorption experiment. Absorption measurements (not shown) were also attempted by Harima et al. [38] for the Ba-rare gas systems with a somewhat different setup. While being in general agreement in shape with our results in the near wings, severe deviations show up at larger detunings, as already noted by Alford et al. [24].

The Ba-He lineshape is not far from being Lorentzian, the main deviation occuring in the blue wing beyond $|\Delta\omega| > 100\,\mathrm{cm}^{-1}$, in which region a satellite structure develops, with a possible maximum beyond $|\Delta\omega| = 500\,\mathrm{cm}^{-1}$. With increasing mass of the perturber the line shapes become increasingly asymmetric. The blue wing satellite is increasingly pronounced, located at approximately 385, 375, 285 and 255 cm^{-1}, respectively. A red wing satellite structure develops gradually, with Ba-Ar showing a diffuse structure in the 10 cm^{-1} region, while Kr and Xe exhibit prominent satellites at about 20 and 35 cm^{-1}, respectively. Their positions shift outwards with increasing mass of the perturber, opposite to the situation in the blue wing.

Generally we note that all Ba-rare gas systems seem to have a far blue-wing satellite (although we were not able to localize it in the case of Ba-He). In addition, the calculated difference potentials for this system [35] display no extreme, and thus no satellites are predicted. This points to the alternative interpretation of an intensity maximum as caused by the Boltzmann factor for the repulsive ground state. Focusing on the differences, we may distinguish between light (He, Ne) and heavy Ba-rare gas systems (Ar, Kr, Xe). In the first group the line shapes have rather smooth, unpronounced features. In the second group line shapes show more dramatic structures, with a minimum in the near blue wing at 10–20 cm^{-1} and a satellite in the red wing.

3.2 Polarizations

Turning to the linear polarization results, we again note increasing structure in the polarizations with increasing perturber mass. For comparison, the polarizations measured for the Sr-rare gas systems [7] are also shown, demonstrating the close similarity between data for the two alkaline earth atoms Sr and Ba, already exploited in the theoretical analysis of Bieniek, Julienne and Rebentrost [12].

The interpretation of the structures in the polarizations and their correlation with structures in the lineshape were presented in detail by Alford et al. [24], with Ba-Xe as a particularly illuminating example, but the same picture holds for Ba-Ar, Kr as well. Briefly, when moving from the impact region at small detunings into the quasistatic wings [24], excitation in the red wing may first take place to both Σ and Π potential curves until a satellite, due to a minimum of the Σ potential curve, is reached near $|\Delta\omega| = 40\,\mathrm{cm}^{-1}$. Since excitation to a Σ curve may yield a larger depolarization than excitation to a Π curve, this explains the corresponding minimum in the polarization data. Going further into the red wing, excitation is now dominantly to a Π curve, giving rise to the increase in polarization in this region. In the blue wing, excitation of the antistatic part [24] at small detunings is accompanied by a rapid drop in polarization, until at larger detunings excitation is predominantly to the Σ curve, yielding a small value for the polarization. At even larger detunings the polarization stays constant, or even increases slightly (in particular for Ba-Xe), presumably due to trajectory effects.

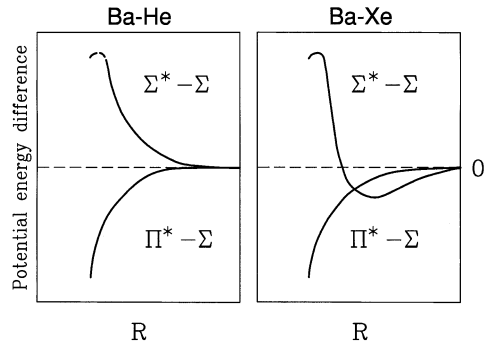

Fig. 8. The potential energy difference between the Σ molecular ground state curve correlating to the BaI 6 ^1S state, and the two molecular excited state curves Σ^* and Π^* correlating to the BaI 6 ^1P state, cf. [35, 24]

For the Ba-He, Ne polarizations we note a smoother variation, and generally higher values than obtained for the heavier rare gas perturbers. In their detailed study of the Sr-Ar polarizations, Bieniek, Julienne and Rebentrost [12] studied the effect of changing the reduced mass of the collision system by replacing Ar with He, keeping the potentials unchanged. In this way they obtained results qualitatively similar to what we find for Ba-He. Furthermore, the recent calculation of potential curves for the Ba-He system [35] hardly displays a minimum in the potential curve difference for the Σ curve, consistent with the absence of a satellite structure in the near red wing. Finally, we recall that when going to lighter systems, the impact regime extends to larger detunings, and that antistatic effects become more important [24, 12].

The main features of the observed line shapes and polarizations may thus be qualitatively interpreted in terms of the different geometries of the relevant potential curve differences, as shown schematically in Fig. 8, with Ba-He and Ba-Xe as the two generic cases. Unfortunately, little direct experimental data presently exists for the Ba-rare gas molecular potential curves. Some spectroscopic information has been obtained for the Ba-Ar system using cold beams [39]; see also [40].

4 Summary and conclusions

Motivated by recent theoretical progress, we have provided far-wing collisional redistribution coefficients and linear polarizations which, together with the data of Alford et al. [24], constitute a complete set for the Ba-rare gas systems. Good agreement is found with experimental results of Alford et al. and blue wing data of Maeyama et al. [37]. Furthermore, the polarizations are very similar

to the corresponding data for the Sr-rare gas systems measured by Alford, Burnett and Cooper [7]. For all parameters, one observes increasing structures when going through the series from He to Xe. The data further corroborates the lineshape-polarization correlations discussed by Alford et al. The systematics observed is in good, qualitative agreement with theoretical predictions of Bieniek, Julienne and Rebentrost [12]. The trends are interpreted in terms of differences in shape of the potential curve differences, as shown in Fig. 8. We hope that this complete set may provide a basis for benchmark calculations based on potential curves evaluated by state-of-the-art pseudopotential methods [36]. In this analysis, circular polarizations should also be included, since they provide an additional, independent check of the consistency of the framework [25].

Finanical support from the Danish Natural Science Research Council and the Carlsberg Foundation is gratefully acknowledged. We thank F. Rebentrost, E. Czuchaj and A. Devdariani for useful communications and the M.Sc. students J. Bak and B. Pállsdottir for contributions to the experimental work. An unknown referee communicated a useful suggestion on the Ba-He lineshape. One of us (NA) acknowledges an invitation from J. Grosser and F. Rebeutrost to the 158. WE Heraeus-Seminar on Atomic Interactions in Laser Fields, which provided an excellent opportunity to discuss the issues on which this paper is based.

References

1. Carlsten, J.L., Szöke, A., Raymer, M.G.: Phys. Rev. A **15**, 1029 (1977)
2. Cooper, J.: Astrophys. J. **228**, 339 (1979)
3. Burnett, K., Cooper, J., Ballagh, R.J., Smith, E.W.: Phys. Rev. A **22**, 2005 (1980); Burnett, K., Cooper, J.: Phys. Rev. A **22**, 2027 (1980); Burnett, K., Cooper, J.: Phys. Rev. A **22**, 2044 (1980)
4. Nienhuis, G.: J. Phys. B **16**, 1 (1983)
5. Burnett, K.: Phys. Rep. **118**, 339 (1985)
6. Thomann, P., Burnett, K., Cooper, J.: Phys. Rev. Lett. **45**, 1325 (1980)
7. Alford, W. J., Burnett, K., Cooper, J.: Phys. Rev. A **27**, 1310 (1983)
8. Lewis, E.L., Harris, M., Alford, W.J., Cooper, J., Burnett, K.: J. Phys. B **16**, 553 (1983)
9. Julienne, P.S., Mies, F.H.: Phys. Rev. A **30**, 831 (1984)
10. Julienne, P.S., Mies, F.H.: Phys. Rev. A **34**, 3792 (1986)
11. Bieniek, R. J.: Phys. Rev. A **35**, 3663 (1987)
12. Bieniek, R. J., Julienne, P.S., Rebentrost, F.: J. Phys. B **24**, 5103 (1991)
13. Kroop, V., Behmenburg, W.: Z. Phys. A **294**, 299 (1980)
14. Havey, M.D., Copeland, G.E., Wang, W.J.: Phys. Rev. Lett. **50**, 1767 (1983)
15. Kulander, K.C., Rebentrost, F.: Phys. Rev. Lett. **51**, 1262 (1983)
16. Kulander, K.C., Rebentrost, F.: J. Chem. Phys. **80**, 5623 (1984)
17. Behmenburg, W., Kroop, V., Rebentrost, F.: J. Phys. B **18**, 2693 (1985)
18. Schuller, F., Nienhuis, G., Behmenburg, W.: Z. Phys. D **2**, 193 (1986)
19. Ermers, A., Woschnik, T., Behmenburg, W.: Z. Phys. D **5**, 113 (1987)
20. Rebentrost, F., Best, R., Behmenburg, W.: J. Phys. B **20**, 2627 (1987)
21. Behmenburg, W., Ermers, A., Rebentrost, F.: Z. Phys. D **18**, 93 (1991)
22. Behmenburg, W.: Phys. Scr. **36**, 300 (1987)
23. Corney, A., McGinley, J.V.M., J. Phys. B **14**, 3047 (1981)
24. Alford, W.J., Andersen, N., Burnett, K., Cooper, J.: Phys. Rev. A **30**, 2366 (1984)
25. Alford, W.J., Andersen, N., Belsley, M., Cooper, J., Warrington, D.M., Burnett, K.: Phys. Rev. A **31**, 3012 (1985)
26. Belsley, M., Cooper, J.: Phys. Rev. A **35**, 1013 (1987)
27. Belsley, M.S., Coutts, J., Cooper, J.: Phys. Rev. A **38**, 3781 (1988)
28. Belsley, M., Alford, W.J., Burnett, K., Cooper, J.: J Quant. Spectrosc. Radiat. Transf. **35**, 53 (1986)
29. Segal, D., Burnett, K.: J. Phys. B **22**, 247 (1989)
30. Bell, I.M., Quayle, C.J.K., Burnett, K.: Phys. Rev. A **47**, 3128 (1993)
31. Grycuk, T., Czerwosz, E.: Physica C **106**, 431 (1981)
32. Findeisen, M., Grycuk, T.: J. Phys. B **22**, 1583 (1989)
33. Czuchaj, E., Stoll, H., Preuss, H.: J. Phys. B **20**, 1487 (1987)
34. Czuchaj, E., Rebentrost, F., Stoll, H., Preuss, H.: Chem. Phys. Lett. **182**, 191 (1991)
35. Czuchaj, E., Rebentrost, F., Stoll, H., Preuss, H.: Chem. Phys. **196**, 37 (1995)
36. Rebentrost, F., Czuchaj, E., Devdariani, A.: Private communications
37. Maeyama, T., Ito, H., Chiba, H., Ohmori, K., Ueda, K., Sato, Y.: J. Chem. Phys. **97**, 9492 (1992)
38. Harima, H., Tachibana, K., Urano, Y.: J. Phys. B **15**, 3679 (1982)
39. Kowalski, A., Funk, D.J., Breckenridge, W.H.: Chem. Phys. Lett. **132**, 263 (1986)
40. Ehrlacher, E., Huennekens, J.: Phys. Rev. A **47**, 3097 (1993)